This article has been accepted for publication in a future issue of this journal, but has not been fully edited. Content may change prior to final publication. Citation information: DOI 10.1109/TIA.2016.2581764, IEEE Transactions on Industry Applications

Universal Restart Strategy for High-Inertia Scalar-Controlled PMSM Drives

Kibok Lee, *IEEE Member*, Sara Ahmed and Srdjan M. Lukic, *IEEE Member*

***Abstract*—In many industrial settings, momentary power disruptions commonly occur, resulting in tripping of large electric machines, which then have to be brought to zero speed before the machine can be restarted. This can result in frequent interruptions in an industrial process, which can have negative effects on productivity. A more practical approach would restart the machine back to the original speed as soon as power is restored, not having to wait for the machine to be at a standstill. This concept is known as flying restart. In this paper we propose an approach to implement the flying restart for permanent magnet synchronous machines (PMSM) by using an identification algorithm which determines the speed and position of the machine back-emf so that the correct voltage vector can be applied, thus minimizing the inrush current during the restart. The novelty of the proposed method is that its implementation only requires nameplate machine parameters and needs no machine-specific tuning, making the approach suitable for implementation with both vector and scalar controlled PMSM.**

***Index Terms*—AC Machines, Position and Speed Estimation, Flying Restart, Permanent Magnet Synchronous Motor (PMSM).**

I. INTRODUCTION

In industrial settings, momentary power interruptions take place due to, for example, temporary power systems faults cleared by relay reclosing, with the interruption lasting as little as tens of milliseconds to a few seconds. In face of such interruptions, industrial machine controllers will typically need to restart from zero speed, requiring total shaft stoppage for the resumption of normal operation. This issue is especially problematic in applications with a large inertia where it may take several minutes for the machine shaft to reach standstill. In such applications, it would be beneficial to resume the machine operation as soon as power is restored.

Methods to determine the machine speed and position have been proposed for induction machines [1-6] and more recently PMSM [7-10]. In the case of IM, the approach in [1-5] proposes the frequency search method using the slip information which does not apply to PMSM. The method in [6] requires an additional voltage sensor to measure the phase voltage. In the case of PMSM, the main drawback shared by methods [7-10] is the requirement that the *d-q* axis stator inductance be known for machine speed and position estimation. This is a major drawback when flying restart is to be applied to scalar-controlled drives where these parameters are generally not known. In [7] the authors estimate the machine speed and position by applying a single zero voltage pulse. The approach in [8], presents a restart method for cylindrical-pole PMSM. This method uses two zero voltage pulses and proposes to compensate the current sampling delay. Methods described in [9, 10] propose using three zero voltage pulses in order to minimize the speed estimation error that can result from a short time interval between two zero voltage pulses. The insertion of the middle pulse helps determine the number of rotations between the pulses. Methods described in [7-10] require the knowledge or estimation of machine parameters for proper operation, which can cause an estimation error if the machine parameters are incorrectly identified, or change due to saturation or temperature effects. Furthermore, in traditional scalar control implementations, considered here, parameters such as the machine *d-q* inductance are generally not known.

An alternate approach to estimate PMSM speed and position uses high frequency current injection [11-15]. In general, high frequency injection methods have been proposed for sensorless vector control and estimate the rotor speed and position even at zero speed. However, these methods require a demodulation process and an observer or a state filter which increases the complexity of restart algorithm. Self-commissioning [16] is another method to determine machine parameters, but this approach is never used in conjunction with scalar control as it would obviate the commissioning simplicity, which is considered one of the main benefits of scalar control.

Generally, the challenges in implementing a restart algorithm for PMSM stems from the fact that (1) the magnetizing flux is always present in PM machines; (2) absence of damper windings can cause machine to lose synchronism; (3) slight error in identifying the speed/position of the back-emf can cause large inrush currents at the beginning of the restart process; and (4) when scalar control is used, machine parameters are typically not available.

In this paper, we propose an effective restart algorithm for high-inertia drives that use scalar control. The proposed approach minimizes the estimation error and eliminates the need for estimating stator inductance, resulting in a universal PMSM restart algorithm. The remainder of this paper explains the state of the art, and presents the principle of operation of proposed restart algorithm in detail. Experimental results are presented to verify the proposed approach.

This article has been accepted for publication in a future issue of this journal, but has not been fully edited. Content may change prior to final publication. Citation information: DOI 10.1109/TIA.2016.2581764, IEEE Transactions on Industry Applications

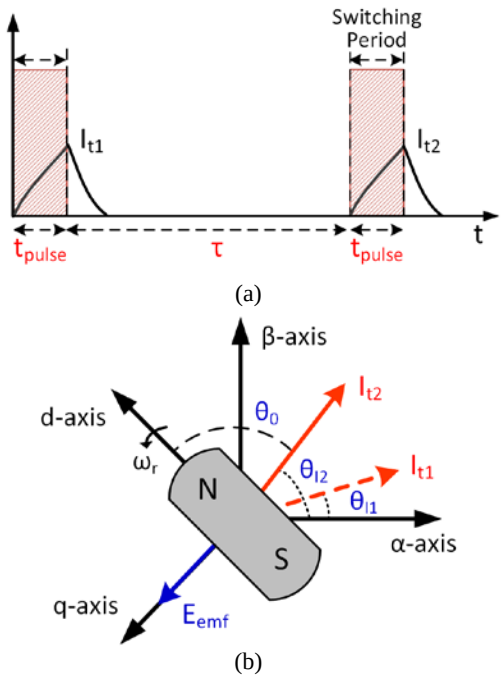

Fig. 1. (a) Two zero voltage pulses and (b) current vectors generated by two zero voltage pulses.

II. Restart Methods for PMSM

We first review the methods for flying restart that have been proposed in the literature. The proposed approach borrows concepts from similar work done on induction machines [1-6] and more recently PMSM [7-10].

A. Rotor Speed Estimation Method

As explained in [8-10, 17] the PMSM rotor speed can be estimated by applying two zero voltage vector pulses, as shown in Fig. 1. The resulting stator phase currents are transformed to the stationary reference frame (I_α, I_β). The angle of each current vector (θ_I) is calculated by using the following equation.

$$\theta_I = tan^{-1}\left(I_\beta / I_\alpha\right) \tag{1}$$

Since the machine inertia is considered to be high, and the time between the two pulses is relatively short, the rotor speed is assumed constant. Therefore, the speed of the rotor can be estimated by using two zero voltage vector pulses, as defined below:

$$\omega_r = \frac{\theta_{I2} - \theta_{I1}}{t_{pulse} + \tau} \tag{2}$$

where t_{pulse} is the time which the zero vector is applied to the stator winding, τ is the time between two pulses, and ω_r is the electrical angular frequency of the rotor. When choosing the delay time (τ), the rated speed of the rotor should be considered so that the interval τ is shorter than the time taken for one electrical revolution [9, 10]. In other words, if the second pulse is applied after the rotor rotates the electric angle 2π [rad], the rotor speed can be estimated incorrectly:

$$\begin{cases} \omega_{real} = \dfrac{\left(\theta_{I2} + 2\pi \cdot N\right) - \theta_{I1}}{t_{pulse} + \tau} & (Actual) \\ \omega_{est} = \dfrac{\theta_{I2} - \theta_{I1}}{t_{pulse} + \tau} & (Estimated) \end{cases} \tag{3}$$

where N is the number of rotations between two pulses, ω_{real} is an actual speed and ω_{est} is the estimated speed using two pulses. The estimated speed will be the same as the actual speed only when N is zero. Therefore, the following equation should be satisfied to prevent incorrect speed estimation.

$$\theta_{I2} - \theta_{I1} = \omega_{real} \cdot \tau < 2\pi \tag{4}$$

In case a rotor direction information is also required, 2π of (4) should be replaced with π.

B. Rotor Position Estimation Method

Equations describing PM machine operation in rotor reference frame is derived from the machine equivalent circuit:

$$\begin{bmatrix} v_d \\ v_q \end{bmatrix} = \begin{bmatrix} R_s + pL_d & -\omega_r L_q \\ \omega_r L_d & R_s + pL_q \end{bmatrix} \begin{bmatrix} i_d \\ i_q \end{bmatrix} + \omega_r \lambda_f \begin{bmatrix} 0 \\ 1 \end{bmatrix} \tag{5}$$

where p denotes the derivative operator, R_s is the winding resistance, v_d & v_q are the d-q axis stator input voltage, i_d & i_q are the d-q axis stator current, L_d & L_q are the d-q axis stator inductance, λ_f is the magnet flux linkage, and ω_r is the electrical angular frequency of the rotor. When applying a zero vector (v_d = 0, v_q = 0), the pulse duration (t_{pulse}) is assumed to be much shorter than the stator time constants (τ_d = L_d/R_s, τ_q = L_q/R_s). In this case, the stator resistance can be neglected. Further validation of this assumption is given in the Appendix. Assuming the stator resistance R_s is negligible, (5) can be simplified to:

$$\begin{bmatrix} 0 \\ 0 \end{bmatrix} = \begin{bmatrix} pL_d & -\omega_r L_q \\ \omega_r L_d & pL_q \end{bmatrix} \begin{bmatrix} i_d(t_{pulse}) \\ i_q(t_{pulse}) \end{bmatrix} + \omega_r \lambda_f \begin{bmatrix} 0 \\ 1 \end{bmatrix} \tag{6}$$

Solving (6) and using Laplace transform, the resulting currents can be calculated as [7, 9, 10]:

$$\begin{bmatrix} i_d(t_{pulse}) \\ i_q(t_{pulse}) \end{bmatrix} = \begin{bmatrix} -\dfrac{\lambda_f}{L_d}\left(1 - \cos \omega_r t_{pulse}\right) \\ -\dfrac{\lambda_f}{L_q} \sin \omega_r t_{pulse} \end{bmatrix} \tag{7}$$

This article has been accepted for publication in a future issue of this journal, but has not been fully edited. Content may change prior to final publication. Citation information: DOI 10.1109/TIA.2016.2581764, IEEE Transactions on Industry Applications

In (7), the rotor speed is considered to be known from (2), t_{pulse} is the duration of the applied zero voltage vector, while *d*-*q* axis stator inductance and λ_f are machine parameters. Thus, *d*-*q* axis rotor reference stator current (i_d & i_q) can be calculated from (7). With this information, the angle difference (θ_0) between the stator current vector angle (θ_I) and the rotor *d* axis angle is found to be:

$$\theta_0 = tan^{-1}\left(i_q / i_d\right) \tag{8}$$

By using position information obtained from (1) and (8), the rotor angle in the stationary reference frame is:

$$\theta_r = \theta_{I2} + \theta_0 . \tag{9}$$

The approach described above, however, has several shortcomings. First, to evaluate the expressions in (7), the *d*-*q* axis stator inductances need to be known. In general, the inductance values are not available in when the machine is driven using scalar control; further, the motor nameplate does not contain this information. Second, the methods in [7-10] are using the PWM switching time as the duty of zero voltage vector. In certain cases, the 100% duty for the zero voltage vector can cause an overcurrent if the machine has a large back-emf (eg. high speed operation or large field flux constant) and a small stator impedance. In fact, this issue occurs for the machine under test in this work, when the machine is operating near the rated speed and the switching frequency is 5kHz or less (see Appendix for details). Third, the θ_0 angle estimation in [7-10] is sensitive to the motor parameter variation and the angle estimation is coupled with the estimated rotor speed. The *d*-*q* axis inductance can vary due to the operating temperature and stator current. Fourth, the error in the sensed current results in incorrect position estimation. The compounding effect of these four drawbacks can result in an incorrect rotor angle (θ_0) estimation, which in turn can lead to an unsuccessful restart by triggering the overcurrent protection.

III. Proposed Restart Method

As described earlier, the goal of this work is to develop an algorithm suitable for scalar control of PMSM that allows the machine to continue operating after a short power outage. In developing the algorithm, we have made the following assumptions: (1) during the power outage, the drive loses power, but the controller does not; (2) the controller has knowledge of the *v*/*f* ratio, and any stabilization loop gains that were in effect during the machine operation prior to the power loss; (3) the controller recognizes the speed command prior to and after the power loss; and (4) the controller monitors the input power (i.e. recognizes when power was lost and when power was restored).

In this section, we present an implementation of flying restart which can be applied universally to any PMSM, assuming that only the nameplate parameters are known.

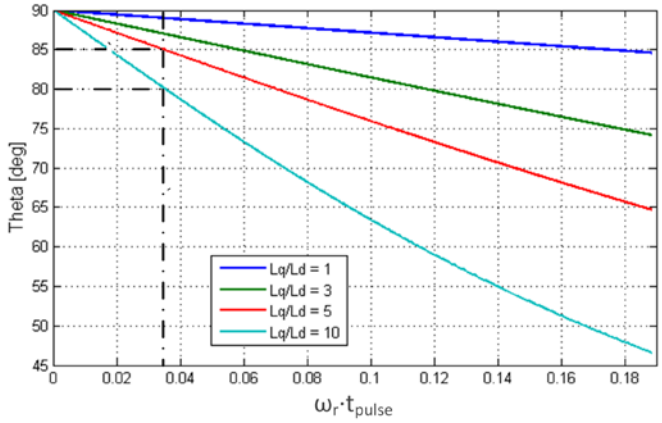

Fig. 2. The angle (θ_0) between the current vector and the rotor position as a function of two variables (L_q/L_d, $\omega_r \cdot t_{pulse}$).

Importantly, this method automatically adjusts the zero vector pulse duty cycle to prevent over-current and adjusts the time between the two pulses considering the rated rotor speed and the acceptable estimation error. We also discuss the resulting speed and the rotor angle estimation error due to current sensing error and motor parameter variation. The proposed method is shown to be less sensitive to both motor parameter variation and current sensing error than the state of the art.

A. Rotor Speed and Position Estimation

To estimate the rotor speed in the proposed restart algorithm, we will use equations (1) and (2), while satisfying condition in (4). To estimate the position, as outlined earlier, we first determine the angle θ_0 between the stator current vector angle θ_I and the rotor *d*-axis angle. Substituting (7) into (8), θ_0 can be determined as:

$$\theta_0 = \tan^{-1}\left(\frac{i_q}{i_d}\right) = \tan^{-1}\left(\frac{L_d}{L_q}\frac{\sin\omega_r t_{pulse}}{1-\cos\omega_r t_{pulse}}\right) \tag{10}$$

Equation (10) is expressed as a function of two variables. One is the inductance ratio (L_q/L_d) and the other is the rotor speed multiplied by the zero vector duration ($\omega_r \cdot t_{pulse}$). The angle between the current vector and the rotor position can be plotted as shown in Fig. 2.

Referring to (10) and Fig. 2, we conclude that for a small zero vector duration ($\omega_r \cdot t_{pulse}$) and a small L_q/L_d ratio, θ_0 approaches 90°. In general, the ratio of *d*-axis and *q*-axis inductance of PMSM is under 5 (see Appendix for more details). Therefore, if $\omega_r \cdot t_{pulse}$ is limited to be below 0.035, the angle between the current vector and the rotor position will always be above 85° [deg.]. As a result, if we assume that θ_0 = 90°, and the conditions above are satisfied, the rotor position estimation error will be less than 5° [deg.]. With this simplification, the position can be calculated from (9) by replacing θ_0 = 90°:

$$\theta_{est} = \theta_{I2} + \pi/2 \tag{11}$$

This article has been accepted for publication in a future issue of this journal, but has not been fully edited. Content may change prior to final publication. Citation information: DOI 10.1109/TIA.2016.2581764, IEEE Transactions on Industry Applications

In our simulations and experiments, we find that the 5° [deg.] position estimation error is acceptable, and results in a minor current spike at startup.

B. *Effect of Current Sensing Error*

We quantify the effect of the current sensing error on the speed estimation. Since the speed estimation is based on the current vector angle (θ_I), an error in current sensing will result in a speed estimation error. Considering that the current sensor can introduce a gain and an offset error, the resulting measured current can be expressed as:

$$\begin{cases} i_{\alpha m} = i_\alpha + \Delta i_{\alpha\_error} + i_{\alpha\_offset} = I_m\left(1+k_\alpha\right)\cos\theta_I + I_{rated}k_{\alpha\_offset} \\ i_{\beta m} = i_\beta + \Delta i_{\beta\_error} + i_{\beta\_offset} = I_m\left(1+k_\beta\right)\sin\theta_I + I_{rated}k_{\beta\_offset} \end{cases} \tag{12}$$

where $i_{\alpha m}$ & $i_{\beta m}$ is the measured α-β axis current, Δi_{α_error} & Δi_{β_error} is α-β axis current error, I_m is the magnitude of current vector, k_α & k_β is the gain error of current sensor and k_{α_offset} & k_{β_offset} is the DC offset percentage (%) of current sensor. In general, the sensor DC offset is compensated before the motor is fed by the inverter. Therefore, the DC offset errors can be ignored in (12). The angle difference between the real current vector and the measured current vector is expressed as [10]:

$$\begin{cases} \theta_I = \tan^{-1}\left(\dfrac{i_\beta}{i_\alpha}\right) \\ \theta_{\mathrm{Im}} = \tan^{-1}\left(\dfrac{i_{\beta m}}{i_{\alpha m}}\right) = \tan^{-1}\left(\dfrac{I_m\left(1+k_\beta\right)\sin\theta_I}{I_m\left(1+k_\alpha\right)\cos\theta_I}\right) \end{cases} \tag{13}$$

Based on (13), and assuming that the current sensor has a 1% sensing gain error, the resulting position error is bound to less than 0.6° [deg.], as shown in Fig. 3. In Fig. 3, the *x*-axis is the current vector angle (θ_I) in the stationary reference frame and *y*-axis is the difference between the actual and estimated position, in face of 1% current sensor gain error. With this result, the maximum speed estimation error is:

$$\omega_{est} = \frac{\theta_{I2} - \theta_{I1}}{N_{delay}\cdot T_{sw}} = \frac{\theta_{\mathrm{Im}2} - \theta_{\mathrm{Im}1} + 2\Delta\theta_{\max}}{N_{delay}\cdot T_{sw}} = \omega_r + \frac{2\Delta\theta_{\max}}{N_{delay}\cdot T_{sw}} \tag{14}$$

Where $\Delta\theta_{max}$ is maximum angle error, N_{delay} is the number of switching cycles (T_{sw}) skipped between the two pulses. Observing (14), it is apparent that the maximum speed estimation error can be controlled by the choice of N_{delay}. The error can then be bounded by the allowable error ε_ω:

$$\frac{2\Delta\theta_{\max}}{\left(\omega_{\max}\varepsilon_\omega\right)T_{sw}} < N_{delay} < \frac{2\pi}{\omega_{\max}T_{sw}}, \tag{15}$$

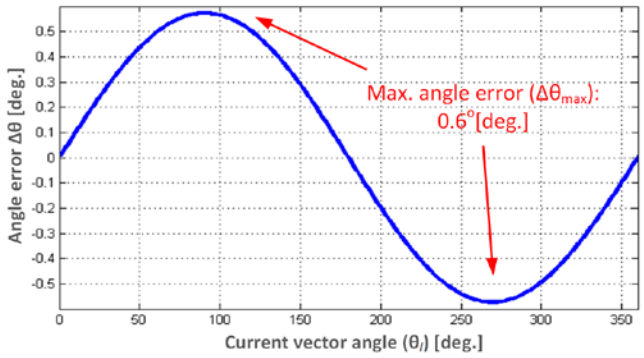

Fig. 3. Current vector angle error caused by 1% current sensing error.

where the upped bound ensures that the delay time does not result in multiple full rotor rotations. In this paper, ε_ω=0.05 (5% error) is considered as a conservative upper bound on the error. Clearly, the speed estimation error can be reduced by increasing N_{delay} in the allowable range.

C. *Quantifying Speed and Position Estimation Errors*

As mentioned before, the methods proposed in [7-10] require the knowledge of machine parameters, which vary with temperature and a stator current. Here, the position estimation error due to L_q inductance variation is investigated. In general, the L_q variation is more critical than L_d variation in the interior permanent motor. To quantify the effect of inductance variation on the position estimate, (7) can be rewritten as:

$$\begin{bmatrix} i_d\left(t_{pulse}\right) \\ i_{q\_actual}\left(t_{pulse}\right) \end{bmatrix} = \begin{bmatrix} -\dfrac{\lambda_f}{L_d}\left(1-\cos\omega_r t_{pulse}\right) \\ -\dfrac{\lambda_f}{\left(L_q+\Delta L_q\right)}\sin\omega_r t_{pulse} \end{bmatrix} \tag{16}$$

where i_{q_actual} is the *q*-axis current changed by the L_q inductance variation ΔL_q. The phase shift θ_0 between the stator current vector angle θ_I and the and the rotor *d*-axis can then be determined by substituting (16) into (8):

$$\theta_{0\_actual} = \tan^{-1}\left(i_{q\_actual}/i_d\right) \tag{17}$$

The actual phase shift θ_{0_actual} determined in (17) will be compared with calculated θ_0 from (8), which was obtained from the nominal value of L_q. Therefore, the position estimation error due to inductance variation is:

$$\Delta\theta_{0\_error} = \theta_{0\_actual} - \theta_0 \tag{18}$$

The error is increased as the L_q variation increases. From (18), the maximum error of the conventional method is 20° [deg.] when the nominal value of L_q varies by 100% [10] (i.e. L_q nominal value is 0.5 or 2).

This article has been accepted for publication in a future issue of this journal, but has not been fully edited. Content may change prior to final publication. Citation information: DOI 10.1109/TIA.2016.2581764, IEEE Transactions on Industry Applications

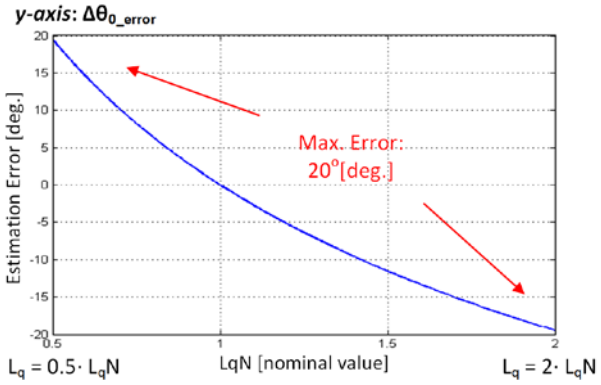

Fig. 4. Rotor position (θ_0) estimation error by q-axis inductance variation in the conventional method [10].

An additional source of error, as described earlier, stems from the estimated rotor speed error (ω_r) caused by the current sensor error, quantified in (14). Referring to (16), the effect of speed estimation error on the position estimation is:

$$\begin{bmatrix} i_{d\_error}(t_{pulse}) \\ i_{q\_error}(t_{pulse}) \end{bmatrix} = \begin{bmatrix} -\frac{\lambda_f}{L_d}\left(1-\cos\left((\omega_r+\Delta\omega_r)t_{pulse}\right)\right) \\ -\frac{\lambda_f}{L_q}\sin\left((\omega_r+\Delta\omega_r)t_{pulse}\right) \end{bmatrix} \quad (19)$$

where $\Delta\omega_r$ is the speed estimation error due to the current sensing error. Finally, considering both inductance variation and current sensing error, the phase shift θ_0 between the stator current vector angle θ_I and the rotor d-axis is found as:

$$\theta_{0\_real} = \tan^{-1}\left(\frac{L_d}{\left(L_q+\Delta L_q\right)}\frac{\sin\left((\omega_r+\Delta\omega_r)t_{pulse}\right)}{1-\cos\left((\omega_r+\Delta\omega_r)t_{pulse}\right)}\right). \quad (20)$$

Due to inductance variation and current sensing error, the rotor position estimation proposed in [7-10] can result in an error exceeding 20° [deg.] when a 100% L_q variation, and 1% current sensing gain error are considered. Fig. 4 shows the calculated position estimation error due to inductance variation, when the approach described in [10] is used. We show experimentally that with an error of this magnitude, the flying restart may fail.

In contrast, the proposed method assumes that the angle (θ_0) between the rotor position and the zero current vector is always 90° [deg.]. Fig. 2 depicts the angle between the rotor position and the zero current vector as the ratio of L_q/L_d changes. This ratio is generally under 5 for PMSM. Considering a 100% variation of L_q, the ratio of L_q and L_d will be under 10, ensuring θ_0 to be above 80° [deg.] as long as $\omega_r \cdot t_{pulse}$ is smaller than 0.035. Therefore, the maximum error of the proposed method will be under 10° [deg.]. In addition, the proposed method does not use the estimated speed to calculate θ_0. Thus, speed estimation error will not affect the angle calculation. As a result, the proposed method is more robust to the L_q inductance variation and speed estimation error than the approaches proposed in the literature.

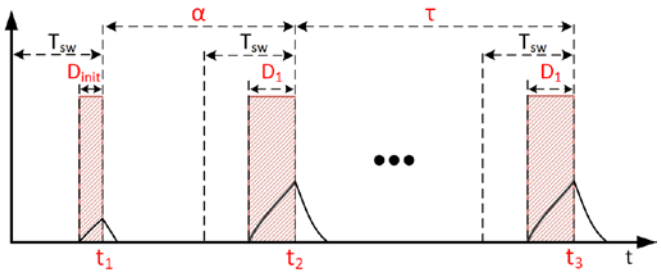

Fig. 5. The overall logic of the proposed restart method.

D. *Implementation of the Proposed Restart Method*

The proposed restart method uses a total three zero voltage pulses to estimate the speed and the position of rotor. Fig. 5 shows the overall estimation procedure using three zero voltage vector pulses. The procedure is explained below.

- Step 1 – Apply the first zero vector pulse with a small duty cycle D_{init} (eg. 10% duty). Record the peak pulse current I_{pulse}. This information will be used to limit the zero vector current and determine the direction of rotation.
- Step 2 – After a time period, α, which satisfies (4), the pulse current will be attenuated to zero. The second zero vector pulse is applied with an adjusted duty (D_1). This duty is selected to limit the resulting pulse current below the rated value and therefore to minimize the breaking torque caused by the resulting current. The angle (θ_{I1}) of the current vector is calculated using (1). The direction of rotation is found based on the information from the first two pulses.
- Step 3 – After a time period τ, a third zero vector pulse is applied. The time period τ is determined from (15), and substituting in for the rated speed and the switching frequency. According to (15) the time period τ can be chosen to make the speed estimation error arbitrarily small. The actual selection of τ should ensure that the machine speed does not significantly change in the interim. Speed and position of the rotor are estimated using (2) and (11).
- Step 4 – If $\omega_r \cdot t_{pulse}$ is a lager than 0.035, the procedure is repeated from step 2 with an adjusted duty, to ensure that this condition is not violated.
- Step 5 – If $\omega_r \cdot t_{pulse}$ is smaller than 0.035 in step 4, the restart is initiated after the stator current reduces to zero.
- Step 6 – The command voltage magnitude is calculated from the back-emf constant, while the applied voltage vector angle is determined from the result of the estimation made in Step 3. The frequency selected for the *v/f* controller is also determined from Step 3. After the voltage is applied to the motor, the stabilizing loop [18] of the *v/f* control starts from the next switching step.

As pointed out, the purpose of first pulse is twofold: (1) to allow a longer time between the second and third pulse by determining the direction of rotation and (2) to estimate the relation between the zero vector pulse duration and peak

This article has been accepted for publication in a future issue of this journal, but has not been fully edited. Content may change prior to final publication. Citation information: DOI 10.1109/TIA.2016.2581764, IEEE Transactions on Industry Applications

current. To determine the relation between the pulse duty cycle and peak current, we assume that the current resulting from the zero vector is linearly increasing. The current slope is derived as:

$$K_{slope} = \frac{E_{emf}}{L_q} = \frac{\Delta I_{pulse}}{\Delta t_{pulse}\left(= D_{init} T_{sw}\right)} \tag{21}$$

Here K_{slope} is the slope of current rise, E_{emf} is back-emf induced by the magnet flux linkage and ΔI_{pulse} is the variation of current magnitude for the duration of the zero voltage vector. The slope of current variation is assumed to be constant because the zero vector is short enough to neglect the stator resistance. Therefore, it is assumed that the current variation is linear and the pulse current is proportional to the duty. The new duty is derived to make the magnitude of the current vector be about one-fifth of the rated current and below the $(\omega_r \cdot t_{pulse}) < 0.035$ limit. Such current will limit the braking torque and overcurrent; but will simultaneously ensure that the sensed current is large enough to minimize the current sensing error.

In the step 3, the switching period delay and the current sampling delay are compensated in the rotor position estimation. The compensated position (θ_{comp}) is obtained as:

$$\theta_{comp} = \theta_{est} + \frac{\omega_{est} T_{sw}}{2} + \omega_{est} T_{sw} \tag{22}$$

The variable θ_{est} is the estimated rotor position calculated in (11). The second term compensates the switching period delay. The third term compensates the current sampling delay.

The proposed method can be applied to any low speed, high inertia PMSM since it only uses the nameplate parameters, and since it automatically limits the current resulting from the zero voltage vector thus preventing an overcurrent. In addition, the positon estimation is robust to inductance variation and current sensor measurement errors.

IV. Experimental Results

A set of experiments was conducted to validate performance of the proposed restart method. Fig. 6 shows that the dynamo test bed consists of a permanent magnet synchronous motor under test, an induction motor for supplying the load torque, a voltage source inverter (VSI) and torque & speed transducer which is used for monitoring a real speed and load torque. The test PM motor parameters are given in Table 1. The inverter used is APS-100T120 fitted with 1200/100A IGBT switches. The selected switching frequency is 5kHz. The *v*/*f* control and the proposed restart method are implemented on the OPAL-RT platform. To implement the control, two current and DC link voltage sensors are used.

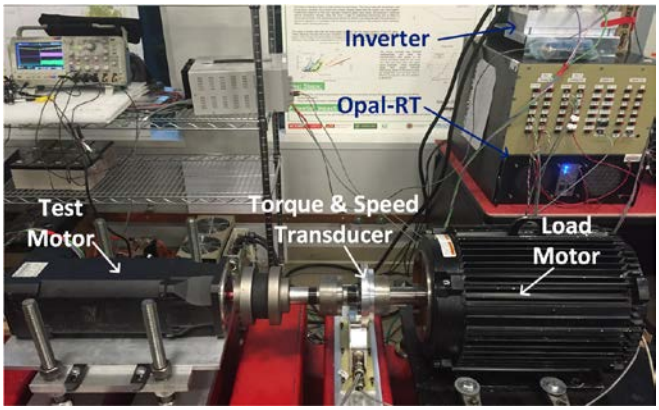

Fig. 6. The dynamo set configuration for the experimental test.

TABLE 1. THE TEST PM MOTOR PARAMETERS

Parameter	Unit	Symbol	Values
Rated Power	[kW]	P_{out}	12
Rated Speed	[rpm]	N_r	3000
Rated Torque	[Nm]	T_e	24
Phase Current (RMS)	[A]	i_s	23.4
Pole	-	n	6
Stator Resistance	[Ω]	R_s	0.12
Stator d-axis Inductance	[mH]	L_d	1.04
Stator q-axis Inductance	[mH]	L_q	1.50
Magnet Flux	[vs/rad]	λ_m	0.29
Inertia	[Nm/rad·s^{-2}]	J	0.059
Bemf (line-line)	[V]	E_{emf}	336

A. Implementation of the Proposed Restart Method

Fig. 7 shows experimental results including the estimated speed and positon of the rotor, the stator current and the actual speed of the transducer when the mechanical rotor speed is 600 and 2400rpm. The restart tests are implemented as follows. First, the motor runs at the defined target speed. The inverter feeding the PM machine is then intentionally powered off for 2 seconds. During this time, the motor speed reduces as a function of the inertia, friction and the load. After 2 seconds, the flying restart algorithm is initiated. Finally, the *v*/*f* control is started with the stabilizing loop [18] and the rotor speed is then brought back to the original reference. The test results of Fig. 7 verify that the proposed restart strategy does not lead to large inrush currents. In addition, the estimated speed (cyan line) is matches well with the real speed (blue line) at restart. The time (τ) between two zero voltage pulses in Fig. 5 was determined from the machine rated speed. For the motor under test, N_{delay} is limited to 33 from (15). The entire restart process is completed in 6.6 ms. This time corresponds to 0.3 rotations of the shaft at the rated speed.

This article has been accepted for publication in a future issue of this journal, but has not been fully edited. Content may change prior to final publication. Citation information: DOI 10.1109/TIA.2016.2581764, IEEE Transactions on Industry Applications

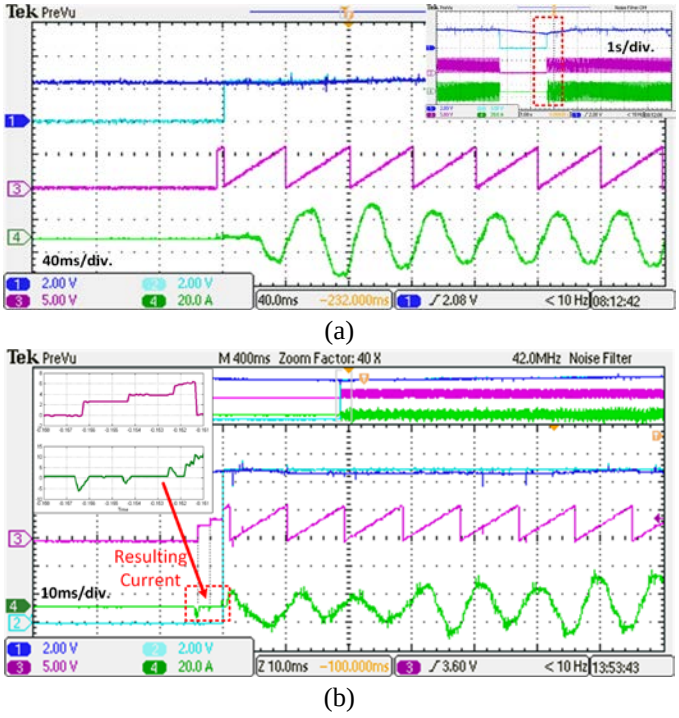

Fig. 7. Restart waveforms (a) 600rpm (b) 2400rpm; CH1: the rotor speed from the transducer (400rpm/div), CH2: the estimated rotor speed (400rpm/div), CH3: the estimated position of the rotor, CH4: the stator phase current (20A/div).

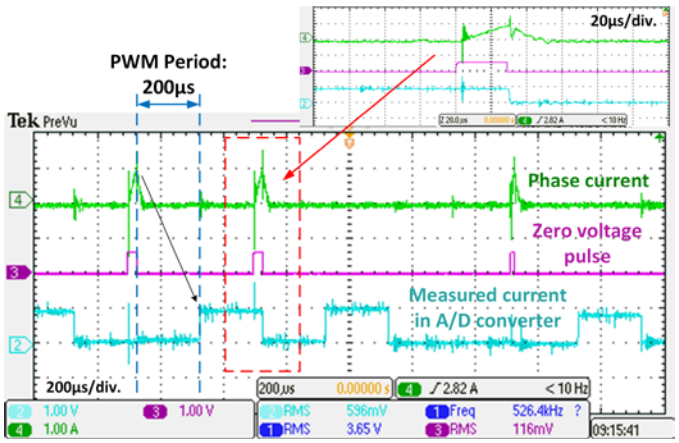

Fig. 8. Phase current resulted by zero voltage pulse and the measured phase current by A/D converter.

Fig. 8 shows the phase current when the zero voltage pulses are applied. The stator current is increases linearly and the slope is determined by the inductance of stator winding. The zero voltage pulse duty is 15% (30µs). The phase current is measured at the end of PWM period using an A/D converter. The current measured by the controller (cyan line) was plotted in next period using a D/A converter in order to show the measurement accuracy.

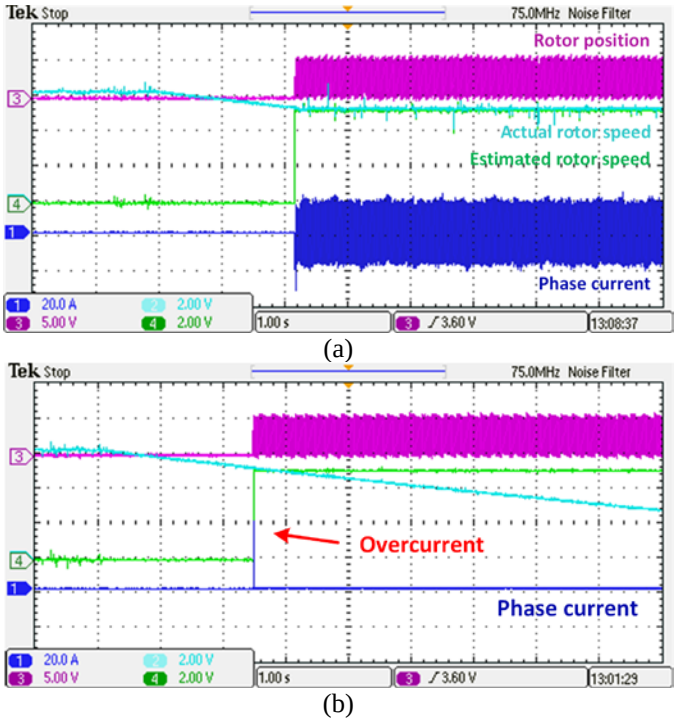

Fig. 9. The theta estimation error tests (a) 15º [deg.] (b) 20º [deg.]; CH1: the phase current (20A/div), CH2: the actual rotor speed (400rpm/div), CH3: the rotor position, CH4: the estimated rotor speed (400rpm/div).

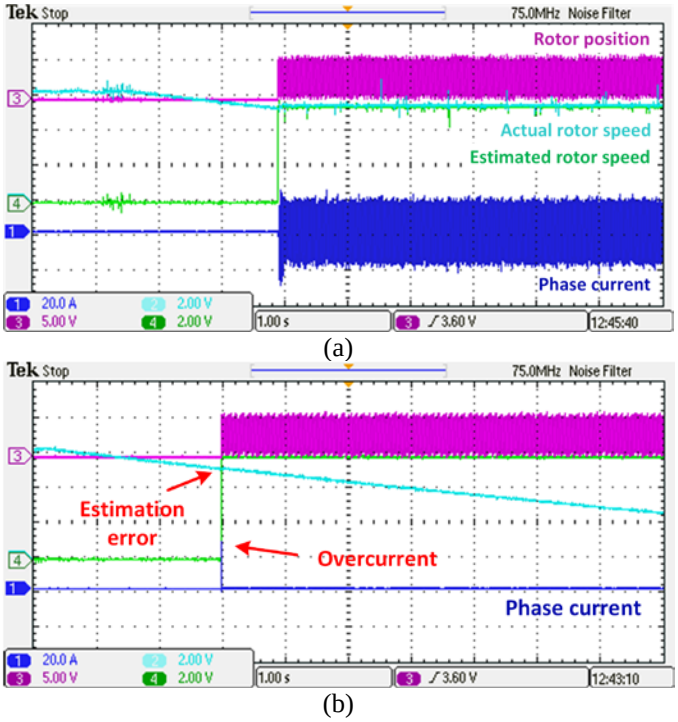

Fig. 10. The speed estimation error tests (a) 5 % (b) 10 %; CH1: the phase current (20A/div), CH2: the actual rotor speed (400rpm/div), CH3: the rotor position, CH4: the estimated rotor speed (400rpm/div).

This article has been accepted for publication in a future issue of this journal, but has not been fully edited. Content may change prior to final publication. Citation information: DOI 10.1109/TIA.2016.2581764, IEEE Transactions on Industry Applications

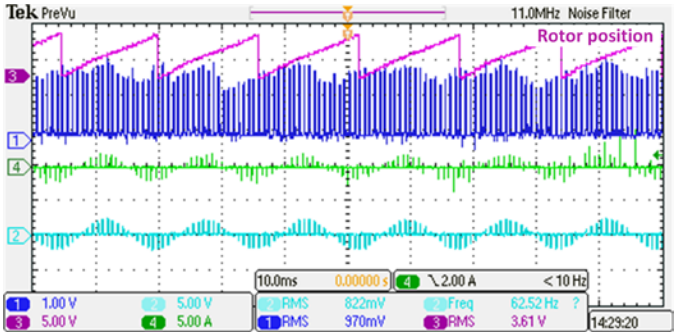

Fig. 11. The effect of current sensor resolution (gain deviation); CH1: the magnitude of current vector (1A/div), CH2: the phase current measured by A/D converter (5A/div), CH3: the estimated rotor position, CH4: the phase current measured by current probe (5A/div).

B. Investigation about the Acceptable Estimation Error

Next, we experimentally investigated the effect of position estimation error on the inrush current. The overcurrent is set to 35A considering the machine rated current. An error is intentionally added to the estimated position and speed, and tests were performed at a speed of 1200rpm. The restart tests are successful up to 15º position error and 5% speed error. When the error exceeds these values, the restart fails due to the overcurrent. Fig. 9 shows the test results done with different theta error conditions (15 and 20º [deg.]). Fig. 10 shows the test results implemented with two different speed error conditions (5 and 10% error of the rotor speed). As a result, the speed and position estimation error should be minimized to prevent the overcurrent.

C. *Issues of Current Sensor Error*

To study the effect of the current sensing error on the position estimation, we performed experiments where the current sensor was intentionally detuned by 1%. The error was introduced in software by changing the sensor gain to correspond to a 1% sensing error. To evaluate the effect of sensor detuning, the machine is spun at a constant speed, and zero voltage pulses of equal duty are applied periodically so that the rotor position can be estimated. Fig. 11 shows the results, where the blue line represents the current measured by the A/D converter, while the magenta line shows the positions estimation. It is clear from the experimental results that the 1% current sensing error affects the position estimation. By analyzing the position estimate off-line (i.e. by looking at the raw data from the oscilloscope), we find the peak error to be 2º. This value is higher than our calculated value of 0.6º, and we attribute the higher error to other sources of noise in the measurement.

V. CONCLUSIONS

The goal of this work was to present a universally-applicable flyback restart algorithm for PM machines. The proposed method uses only the nameplate machine parameters. In general, the nameplate parameters do not include the information such as *d-q* axis stator inductance, which are needed for other methods proposed in the literature. The approach is best suited for application in high-inertia system, due to the assumption that the rotor speed is near-constant during the restart process. This assumption is acceptable, since the restart function is used in high inertia application, where reaching standstill may take a relatively long time. We show that the maximum positon estimation error of the proposed method is smaller than that of the existing method used in [10] in presence of inductance and rotor speed estimation errors. Experimental results presented validate the performance of the proposed restart method.

APPENDIX

Table 2 lists motor parameters of commercial PMSMs. Motors #1~4 were used in the reference papers while Motors #5 and #6 are manufactured by ABB. In order to validate our assumption that keeping the product $\omega_r \cdot t_{pulse}$ below 0.035, we calculate the resulting duty cycle and the resulting current as a percentage of the rated value, when the machine speed is at the rated value (i.e. under worst-case conditions). We conclude that the duty cycle can be actuated by the controller, and the resulting current is large enough to be measured with the 1% allowable error which would cause up to 0.6º[deg.] error in the position estimation, as demonstrated in Fig. 3.

We also evaluate if the assumption that the rotor resistance can be neglected is valid for the proposed duty cycles of the zero pulse vectors. The current vector angles (θ_0) are calculated from both (5) and (6), i.e. with and without ignoring the stator resistance. Current vector angles for the two cases are plotted in the top plot of Fig. 12. The bottom plot shows the difference between two current vector angles as a function of the ratio of zero vector pulse time (t_{pulse}) to the machine electrical time constant (τ_q). We note that the largest ratio of t_{pulse}/τ_q in Table 2 is 0.3%, which results in negligible position error. Referring to Fig. 12, even if t_{pulse}/τ_{el}=10% the position error will only reach 1%. Finally, in Table 2, we note that the largest ratio of L_q/L_d for the motors considered is 4. This supports our assumption that L_q/L_d is typically below 5.

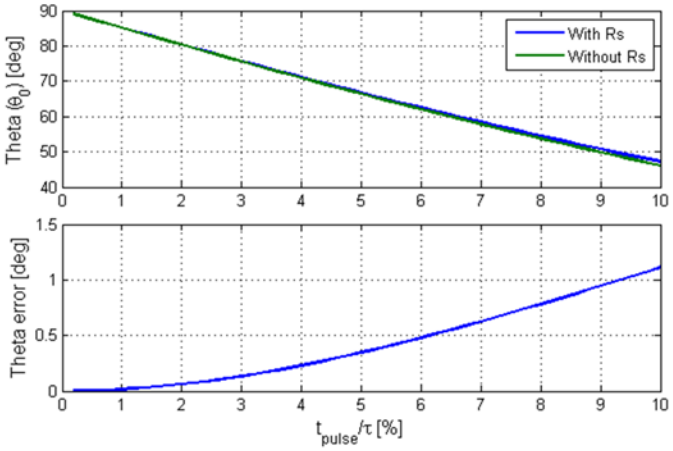

Fig. 12. The effect by the stator resistance neglect while deriving current vector angle (θ_0) of (8).

This article has been accepted for publication in a future issue of this journal, but has not been fully edited. Content may change prior to final publication. Citation information: DOI 10.1109/TIA.2016.2581764, IEEE Transactions on Industry Applications

TABLE 2. MOTOR PARAMETERS OF COMMERCIAL PMSMS

Parameter	Unit	Motor #1 [10]	Motor #2 [18]	Motor #3 [19]	Motor #4 [20]	Motor #5	Motor #6	Test Motor
Rated Power	[kW]	2	2.2	3.7	3.7	412	186	12
Rated Speed	[rpm]	2,100	1,750	2,000	1,800	1,800	125	3,000
Rated Torque	[Nm]	9	12	17.67	20	1,612	10,481	24
Rated Current	[A]	15	4.1	5.8	14	665	325.3	23.4
Pole	-	4	6	4	6	4	8	6
Stator R	[Ω]	0.248	3.3	2.0	0.348	0.002	0.042	0.12
Stator d-axis L	[mH]	8	41.59	33	3	0.171	8.29	1.04
Stator q-axis L	[mH]	32	57.06	96	14.9	0.5663	20.96	1.50
Magnet Flux	[vs/rad]	0.367	0.48	0.68	0.22	0.55	3.27	0.29
Inertia	[kg.m^2]	5.35	10.07*10e-3	-	0.01	21	40	0.06
PWM	[kHz]	1	5	8	4	4	4	5
Condition: $\omega_r = \omega_{rated}$, $t_{pulse} = 0.035/\omega_{rated}$								
I/ I_{rated}	[%]	2.67	7.18	4.28	3.76	5.09	1.68	28.92
Pulse Duty	[%]	8	32	37	25	267	67	19
Ratio of L_q/L_d	-	4.00	1.37	2.91	2.50	3.31	2.53	1.44
$\tau_q = L_q/R_s$	[s]	0.129	0.017	0.048	0.043	0.283	0.500	0.013
t_{pulse}/τ_q	[%]	0.06	0.37	0.17	0.14	0.03	0.13	0.30

REFERENCES

[1] P. Hangwen, L. Springob and J. Holtz, "Improving the start and restart behavior through state recognition of AC drives," in *Power Conversion Conference* , Nagaoka, 1997, pp. 589-594.

[2] H. Iura, K. Ide, T. Hanamoto and Zhe Chen, "An Estimation Method of Rotational Direction and Speed for Free-Running AC Machines Without Speed and Voltage Sensor," Industry Applications, IEEE Transactions On, vol. 47, pp. 153-160, 2011.

[3] A. David, E. Lajoie-Mazenc and C. Sol, "Maintaining the synchronism of an AC adjustable speeddrives during short supply interruptions for an optimal and automatic soft restart," in Industrial Electronics, 1993. Conference Proceedings, ISIE'93 - Budapest., IEEE International Symposium on , 1993, pp. 463-470.

[4] A. David, E. Lajoie-Mazenc and C. Sol, "Soft restart of an adjustable speed drive after a short disconnection without any mechanical speed sensor," in Electrical Machines and Drives, 1993. Sixth International Conference on (Conf. Publ. no. 376) , 1993, pp. 570-575.

[5] K. Suzuki, S. Saito, T. Kudor, A. Tanaka and Y. Andoh, "Stability improvement of V/F controlled large capacity voltage-source inverter fed induction motor," in Industry Applications Conference, 2006. 41st IAS Annual Meeting. Conference Record of the 2006 IEEE, 2006, pp. 90-95.

[6] Se-Jong Jeong, Young-Min Park and Gi-Jun Han, "An estimation method of rotation speed for minimizing speed variation on restarting of induction motor," in *Power Electronics and ECCE Asia (ICPE & ECCE), 2011 IEEE 8th International Conference On*, 2011, pp. 697-704.

[7] Takuya Horie and Keiichiro Kondo, "Experimental Study on a Restarting Procedure at Coasting Condition for a Rotational Angle Sensorless PMSM," IEEJ Journal of Industry Applications, vol. 3, pp. 131-137, 2014.

[8] Y. C.Son, S.-J. JANG and R. D. Nasrabadi, "Permanent magnet AC motor systems and control algorithm restart methods," US8054030 B2, Nov 8, 2011.

[9] Toshifumu Y., Shinji W., Keiichiro K., Takashi Y., Shun T. and Shinsuke M, "Starting Procedure of Rotation Sensorless PMSM at Coasting Condition for Railway Vehicle Traction," Electrical Engineering in Japan, vol. 169, 2009.

[10] S. Taniguchi, S. Mochiduki, T. Yamakawa, S. Wakao, K. Kondo and T. Yoneyama, "Starting Procedure of Rotational Sensorless PMSM in the Rotating Condition," Industry Applications, IEEE Transactions On, vol. 45, pp. 194-202, 2009.

[11] Lin, T.C.; Zhu, Z.Q., "Sensorless operation capability of surface-mounted permanent magnet machine based on high-frequency signal injection methods," Industry Applications, IEEE Transactions On, vol. 51, pp. 2161-2171, 2015.

[12] Lin, T.C.; Zhu, Z.Q., "Novel Sensorless Control Strategy With Injection of High-Frequency Pulsating Carrier Signal Into Stationary Reference Frame," Industry Applications, IEEE Transactions On, vol. 50, pp. 2574-2583, 2014.

[13] Sungmin Kim; Jung-Ik Ha; Seung-Ki Sul, "PWM Switching Frequency Signal Injection Sensorless Method in IPMSM," Industry Applications, IEEE Transactions On, vol. 48, pp. 1576-1587, 2012.

[14] Murakami, S.; Shiota, T.; Ohto, M.; Ide, K.; Hisatsune, M., "Encoderless Servo Drive With Adequately Designed IPMSM for Pulse-Voltage-Injection-Based Position Detection," Industry Applications, IEEE Transactions On, vol. 48, pp. 1922-1930, 2012.

[15] ShihChin Yang; Lorenz, R.D., "Comparison of resistance-based and inductance-based self-sensing controls for surface permanent-magnet machines using high-frequency signal injection," Industry Applications, IEEE Transactions On, vol. 48, pp. 977-986, 2012.

[16] Odhno, S.A.; Giangrande, P.; Bojoi, R.I.; Gerada, C., "Self-Commissioning of Interior Permanent- Magnet Synchronous Motor Drives With High-Frequency Current Injection," Industry Applications, IEEE Transactions On, vol. 50, pp. 3295-3303, 2014.

[17] Yoo, H.; Jang-Hwan Kim; Seung-Ki Sul, "Sensorless Operation of a PWM Rectifier for a Distributed Generation," Power Electronics, IEEE Transactions on, vol. 22, pp. 1014-1018, 2007.

[18] P. Chandana Perera, F. Blaabjerg, J. K. Pedersen and P. Thogersen, "A sensorless, stable V/f control method for permanent-magnet synchronous motor drives," Industry Applications, IEEE Transactions On, pp. 783-791, 2003.

[19] A. Consoli, G. Scelba, G. Scarcella, and M. Cacciato, "An effective energy saving scalar control for industrial IPMSM drives," IEEE Trans. Industry Electron., vol. 60, pp. 3658-3669, 2013.

[20] Itoh J.-I., Nomura N., Ohsawa H.: 'A comparison between V/f control and position-sensorless vector control for the permanent magnet

synchronous motor'. Proc. Power Conversion Conf. PCC Osaka 2002, Osaka, Japan, April 2002, vol. 3, pp. 1310–1315

Kibok Lee (S'13–M'15) received the B.S. and M.S. degrees in electrical engineering from Korea University, Seoul, Korea, in 2005 and 2007, respectively, and the Ph.D. degree in electrical engineering from North Carolina State University, Raleigh, NC, USA, in 2016.

From 2007 to 2011, he was a Research Engineer with LG electronics R&D Center, Seoul, Korea, where he was involved with the development of AC motor drives. Since 2016, he has been with the General Motors Powertrain Center, Pontiac, MI, where he works on motor control for vehicle applications. His current research interests include motor drives, power conversion system and inductive power transfer system.

Sara Ahmed received the B.S degree in electrical engineering from Virginia Polytechnic Institute and State University (Virginia Tech), Blacksburg, in 2006. In 2006, she joined the Center for Power Electronics Systems as a direct Ph.D. Student at Virginia Tech and received the M.S. and Ph.D. degrees in 2007 and 2011, respectively. In 2011, she joined ABB Corporate Research, Raleigh, NC, where she became a Senior Scientist in 2015. Her research interest include modeling, simulation and stability of power electronic systems and design and control of three phase converters and AC drives.

Srdjan M. Lukic (S'02–M'07) received the Ph.D. degree in electrical engineering from the Illinois Institute of Technology, Chicago, IL, USA, in 2008. He is currently an Associate Professor with the Department of Electrical and Computer Engineering, North Carolina State University, Raleigh, NC, USA. He serves as the Distributed Energy Storage Devices Subthrust Leader of the National Science Foundation Future Renewable Electric Energy Delivery and Management (FREEDM) Systems Engineering Research Center, North Carolina State University. His current research interests include design, and control of power electronic converters and electromagnetic energy conversion with application to wireless power transfer, energy storage systems, and electric automotive systems. Dr. Lukic serves as an Associate Editor of the IEEE Transactions on Transportation Electrification. He has served as a Guest Editor of the Special Section of the IEEE Transactions on Industrial Electronics on Energy Storage Systems—Interface, Power Electronics and Control. He is a Distinguished Lecturer with the IEEE Vehicular Technology Society from 2011 to 2015.